RSC Medicinal Chemistry

ROYAL SOCIETY OF CHEMISTRY

RESEARCH ARTICLE

View Article Online
View Journal

Cite this: DOI: 10.1039/d5md00589b

Design and synthesis of photoswitchable desloratadine ligands for histamine H_1 receptor photopharmacology

Lars C. P. Binkhorst, † Ivana Josimovic,† Daan de Vetten, Tyrone J. Nijman, Niels J. Hauwert, Sufyan Ahmad, Oscar P. J. van Linden, Iwan J. P. de Esch, Henry F. Vischer, Maikel Wijtmans * and Rob Leurs*

Despite the pharmacological relevance of the histamine H_1 receptor (H_1R), the second most therapeutically targeted G protein-coupled receptor (GPCR), an effective photoswitchable ligand to optically control this receptor remains elusive. In this work, we aimed to identify a suitable photoswitchable H_1R ligand by performing an 'azoscan' on the H_1R antagonist desloratadine. Taking advantage of the synthetic toolbox available for the desloratadine scaffold, aniline groups were regioselectively installed on the aromatic positions of this scaffold to enable the synthesis of azobenzene analogs targeting the orthosteric binding pocket of H_1R. Additionally, we functionalized the piperidine ring of desloratadine with azobenzene moieties. These two strategies resulted in a total of nine photoswitchable compounds, displaying efficient *trans* to *cis* isomerization (PSS_{cis} > 87%) and a broad range of thermal relaxation half-lives. Pharmacological evaluation revealed the 2-position (**10a**) to be most suitable for accommodation of a photoswitchable group, as it exhibits the most balanced profile in absolute affinity (K_i *trans* = 2 nM) and a 3.2-fold light-induced affinity shift. Computational docking studies provide a rationale, with the binding pose of the *trans* and *cis* isomer in the H_1R binding pocket potentially being inverted. While the development of effective photoswitchable ligands for H_1R remains challenging, this study provides promising opportunities for future optimization to achieve optical control of this GPCR.

Received 7th July 2025,
Accepted 13th August 2025

DOI: 10.1039/d5md00589b

rsc.li/medchem

Introduction

Photopharmacology enables precise spatiotemporal control of protein function using light, offering powerful tools to investigate dynamic signaling processes.[1] Photopharmacology uses photoresponsive ligands,[2] employing one of two main strategies: (i) photocaging, which uses ligands with photocleavable protecting groups[3] or (ii) photoswitching, which uses small-molecule ligands that undergo light-induced isomerization.[1,4,5] Successful design of photoswitchable ligands requires incorporation of a photoswitchable moiety (often an azobenzene) in such a way that the two isomers have different pharmacological properties. This can be achieved by (i) azologization, where a bioisoster (azosteres) in the core of the template ligand is replaced by an azobenzene or (ii) azoextension, where the template ligand is expanded with a photoswitchable unit.[5,6]

Photoswitchable ligands have been developed for a broad range of biological targets, including ion channels, enzymes and G protein-coupled receptors (GPCRs).[6,7] GPCRs represent one of the most pharmacologically relevant protein families, with approximately 36% of the approved drugs targeting GPCRs.[8] After the dopamine D_2 receptor, the histamine H_1 receptor (H_1R) is the second most frequent GPCR targeted by approved drugs, with 59 drugs targeting this receptor.[8] H_1R is widely distributed throughout the body, in, for example, smooth muscle cells, endothelial cells and the central nervous system. H_1R antagonists, also known as antihistamines, are a class of drugs used to treat allergic diseases like allergic rhinitis, allergic conjunctivitis, and urticaria.[9] These drugs alleviate symptoms such as itching, swelling, and redness by blocking the action of histamine on the H_1R. Despite significant progress in the GPCR photopharmacology field,[10–13] and the high number of drugs targeting H_1R,[8] it has proven remarkably difficult to develop a photoswitchable ligand that effectively modulates this receptor. Rustler *et al.* previously published photoswitchable ligands targeting guinea pig H_1R (gpH_1R)[14] based on a clozapine derivative (**1**, Fig. 1A).[15] However, the resulting photoswitchable compounds **2** and **3** exhibit low affinity for gpH_1R and no data on human H_1R

Amsterdam Institute of Molecular and Life Sciences, Division of Medicinal Chemistry, Faculty of Science, Vrije Universiteit Amsterdam, De Boelelaan 1083, 1081 HV Amsterdam, The Netherlands. E-mail: m.wijtmans@vu.nl, r.leurs@vu.nl
† Authors contributed equally to this manuscript.

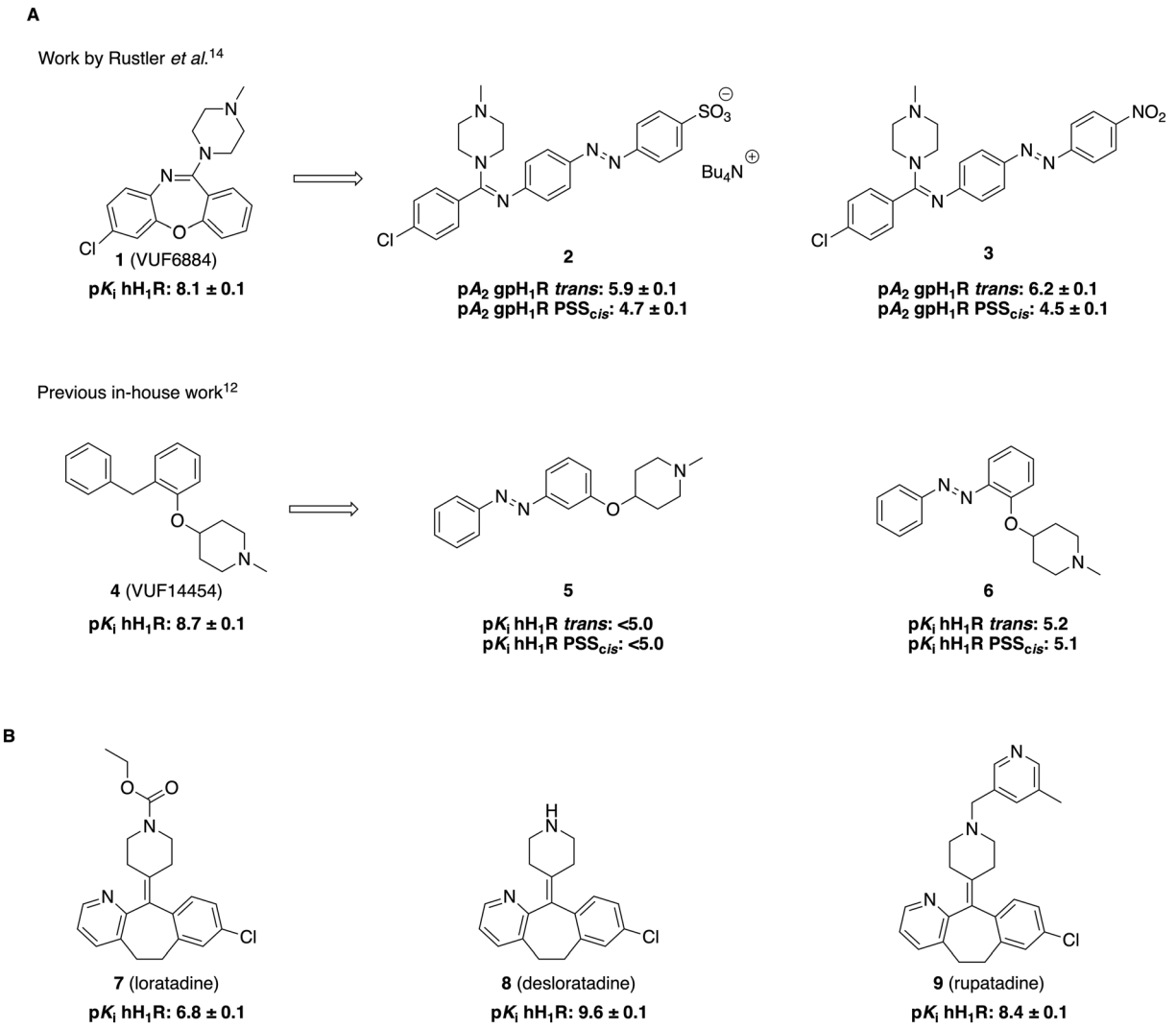

Fig. 1 Structures and pharmacological data of key compounds. Except for **2** and **3**, in-house affinity data and associated references are provided. (A) Previously reported photoswitchable ligands targeting gpH_1R[14] based on **1** (VUF6884)[15] or targeting hH_1R[12] based on **4** (VUF14454)[16] (B) structures of loratadine,[23] desloratadine (value from Table 2) and rupatadine.[24]

(hH_1R) were disclosed. Previous in-house efforts with photoswitchable molecules **5** and **6** based on VUF14454 (**4**)[16] were also unsuccessful with the ligands having low H_1R affinity and no appreciable affinity shift between isomers.[12] Likewise, the desmethyl analog[16] of these compounds or substitution of the nitrogen atom with an acidic moiety connected through a linker,[17] were ineffective (unpublished data). Thus, an effective photoswitchable hH_1R ligand remains elusive to date. We reasoned that the 11-(piperidin-4-ylidene)-6,11-dihydro-5*H*-benzo[5,6]cyclohepta[1,2-*b*]pyridine core, as in antihistamines loratadine (**7**, Fig. 1B) and desloratadine (**8**), provides a promising scaffold. Both are well-characterized compounds that are frequently used in exemplification for late-stage aromatic functionalization.[18–22] In the current work, we capitalized on this synthetic accessibility by performing an 'azoscan' on desloratidine, a unique approach in which the azobenzene moieties are systematically installed on different positions of the template scaffold to identify a suitable position for placement of a photoswitchable moiety. These include aromatic vectors, but also *N*-substitution on the piperidine ring, generating analogs of rupatadine (**9**).

Results and discussion

Design

The design of new photoswitchable ligands targeting hH_1R (Fig. 2) is based on the second-generation antihistamine desloratadine (**8**) as the template. It exhibits an approximately 600-fold higher affinity for hH_1R than loratadine (**7**, Fig. 1B).[23,24] The cryo-EM structure of desloratadine bound to hH_1R, published by Wang *et al.*,[25] has revealed that it engages in key hydrogen bond interactions with $D107^{3.32}$ and $Y431^{6.52}$ within the orthosteric hH_1R pocket. The structure suggests that there is space for growth on desloratadine, particularly on the side of the pyridine ring (Fig. S1). Notably, Wang *et al.* also found that the ligand-binding pocket of H_1R

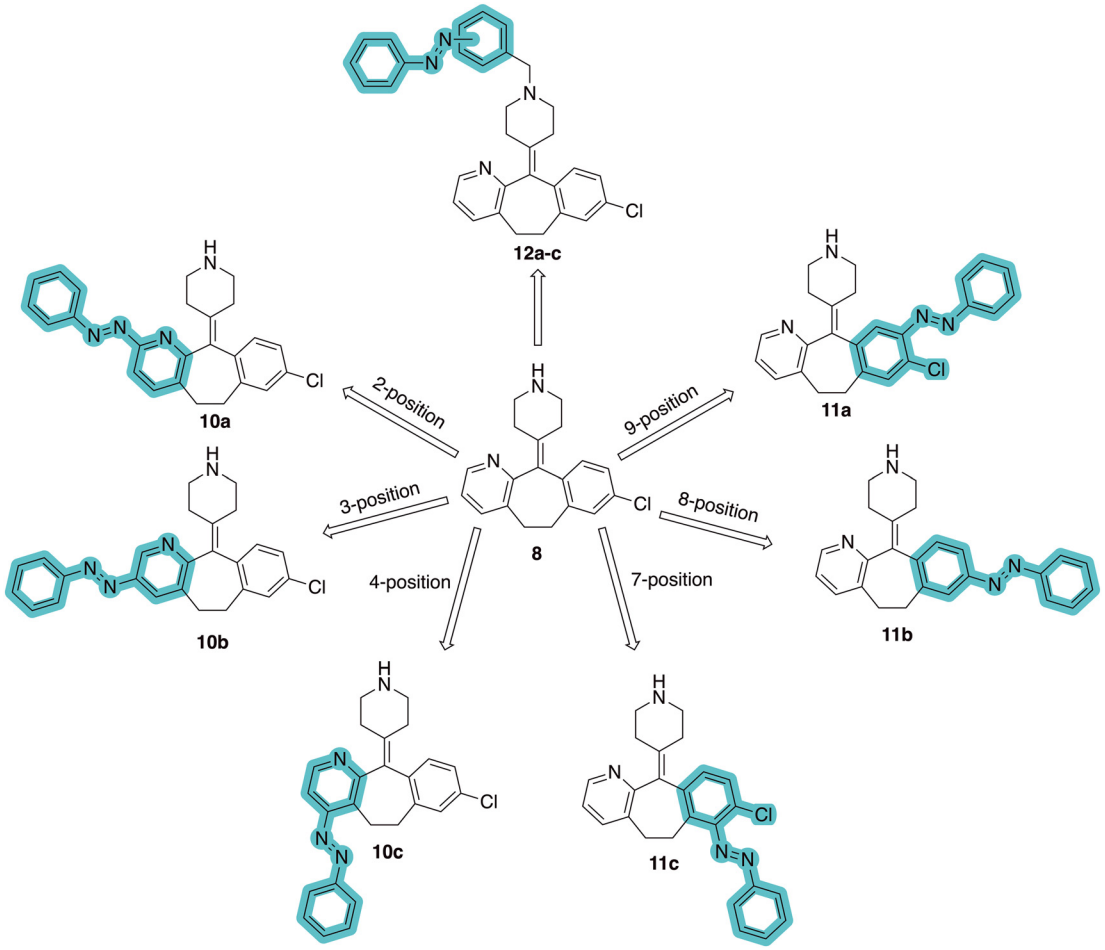

Fig. 2 Design strategy towards a photoswitchable hH_1R ligand by performing an 'azoscan' on desloratadine (**8**).

shows significant conformational flexibility based on the ligand bound, offering additional opportunities to potentially accommodate a photoswitchable ligand in the orthosteric pocket.[25]

The 11-(piperidin-4-ylidene)-6,11-dihydro-5*H*-benzo[5,6]cyclohepta[1,2-*b*]pyridine core of desloratadine has proven compatible with several late-stage synthetic functionalization approaches.[18–22] We hypothesized that the use of such literature approaches would enable the installation of aniline moieties on the pyridine and phenyl rings, thereby providing synthetic vectors for the subsequent formation of an azo bond. Leveraging this synthetic accessibility, we conducted a systematic 'azoscan'. By introducing azobenzene moieties at various positions of desloratadine, we sought to identify a photoswitchable ligand where one isomer has a favorable conformation within the binding site, while the other isomer induces steric clashes and/or unfavorable interactions to induce an affinity shift. In total, three series were explored (Fig. 2). The first two series involve introduction of an azobenzene on the pyridine ring on the 2-, 3-, and 4-positions (**10a–c**) and at the phenyl ring on the 7-, 8-, and 9-positions (**11a–c**) to target the orthosteric binding pocket. Substitution of the 8-position required removal of the chlorine of desloratadine. Importantly, Lall *et al.* have shown that replacement of the chlorine atom of loratadine with a hydrogen atom results in an equipotent compound.[26] Furthermore, we did not pursue the 10-position, located on the phenyl ring, due to the significant synthetic challenges expected with this sterically hindered position. The third series we explored is substitution at the piperidine ring (**12a–c**), *i.e.*, based on rupatadine as a template.

Synthesis

The synthesis routes for the first two series of photoswitchable desloratadine analogs (**10a–c**, **11a–c**) were designed to regioselectively install aniline groups on the aromatic rings (Scheme 1), enabling subsequent azobenzene formation. For the preparation of the 2-isomer (**10a**), desloratadine (**8**) was first protected to give Boc-protected intermediate **13**, which was oxidized with *m*-CPBA to *N*-oxide **14**. *ortho*-Amination, following the method of Verbeet *et al.*,[27] yielded aminopyridine **15**. Subsequent formation of the azobenzene using PhNO under acidic Mills conditions afforded azobenzene **16**, which was deprotected with HCl to yield **10a**. Intermediate **14** was also used for the preparation of the 4-isomer (**10c**). Substitution of the hydrogen atom through a triflate-intermediate, based on a procedure by Choi *et al.*,[28] gave intermediate **17**. Due to poor

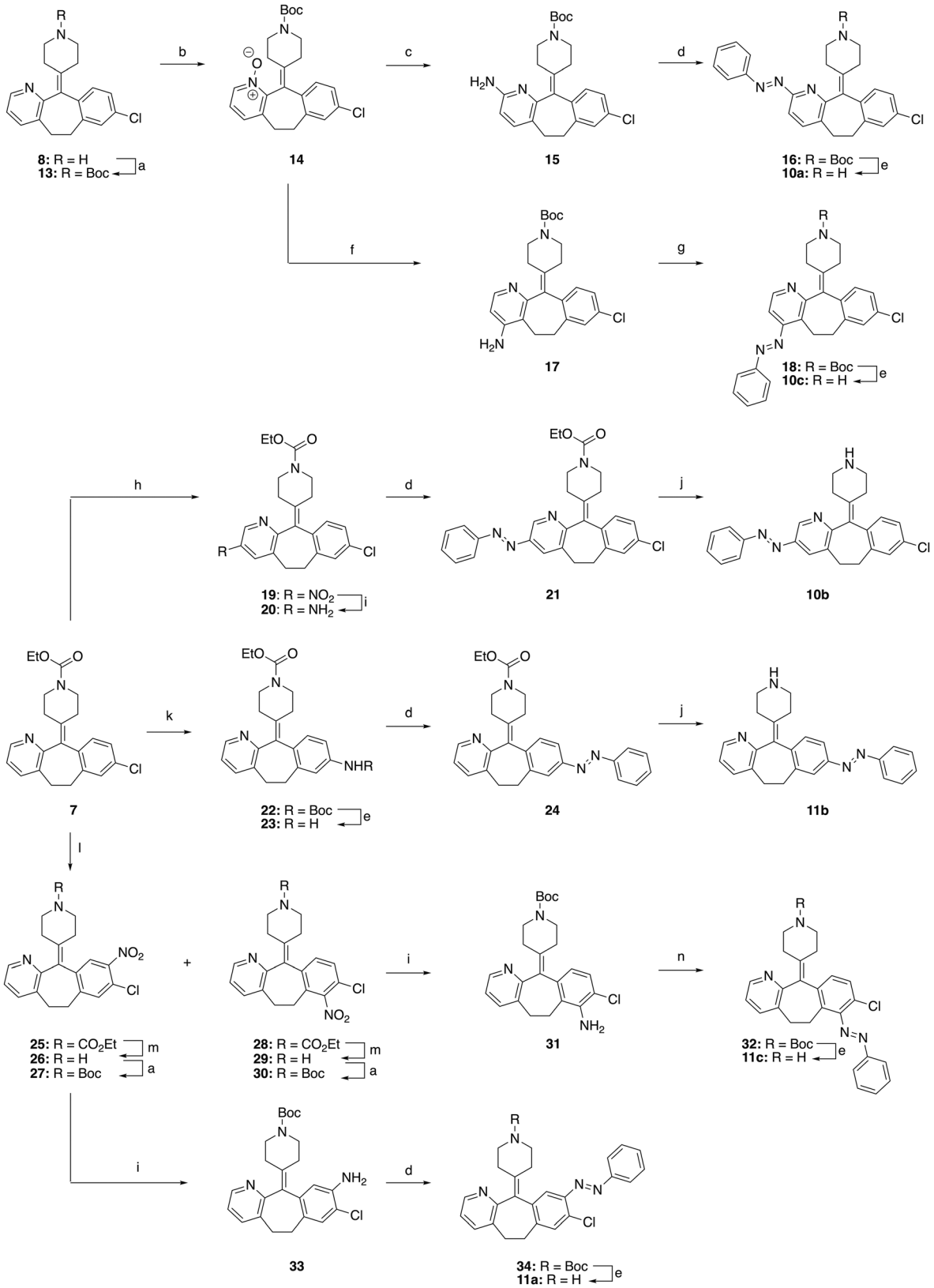

Scheme 1 Synthesis of **10a–c** and **11a–c**. Reagents and conditions: (a) Boc_2O, Et_3N, DCM, rt, 2–16 h, 82–95%; (b) *m*-CPBA, DCM, rt, 50 min, 61%; (c) (i) potassium phthalimide, TsCl, Et_3N, DCM, rt, 20 h; (ii) $H_2NNH_2{\cdot}H_2O$, H_2O, 63%; (d) PhNO, AcOH, PhMe, 18 h–14 d, 75–90 °C, 8–36%; (e) 4 M HCl in 1,4-dioxane, MeOH, rt, 16–22 h, 16–98%; (f) (i) 4-cyanopyridine, Tf_2O, DCM, MeCN, 0 °C to rt; (ii) Aq. NH_4OH, rt, 16 h, 25%; (g) PhNO, NaH, THF, rt, 72 h, 23%; (h) Bu_4N^+ NO_3^-, TFAA, DCM, rt, 66 h, 21%; (i) Fe, NH_4Cl, 1,4-dioxane, EtOH, H_2O, 80 °C, 2–3 h, 81–89%; (j) KOH, EtOH, H_2O, 80 °C, 72–100 h, 33–61%; (k) XPhos, $Pd(OAc)_2$, $BocNH_2$, Cs_2CO_3, 1,4-dioxane, 95 °C, 2 h, 82%; (l) Conc. H_2SO_4, KNO_3, –10 °C – rt, 16 h, 81% of **25** and 9% of **28**; (m) Conc. HCl, 80 °C, 24 h, 82–89%; (n) (i) $BF_3{\cdot}Et_2O$, *t*-$BuNO_2$, THF, rt, 2 h; (ii) PhMgBr, THF, –70 °C, 18 h, 14%.

reactivity of this intermediate in the Mills reaction under acidic conditions, the aniline was rendered more nucleophilic by deprotonation successfully providing **18.** Deprotection of the Boc group in **18** with HCl afforded **10c**. The 3-isomer was synthesized *via* regioselective nitration of loratadine (**7**).[29,30] Reduction of the resulting nitro-compound **19** *via* a Béchamp reduction provided aniline **20**, which was subjected to acidic Mills conditions (affording **21**) and carbamate deprotection with KOH to yield **10b**.

For installation of the azobenzene at the 8-position (**11b**), a Buchwald–Hartwig amination of loratadine (**7**) with *tert*-butylcarbamate yielded **22**. Boc-deprotection to **23** followed by the Mills reaction under acidic conditions afforded intermediate **24**, which was deprotected using KOH to give **11b**. The 7- and 9-analogs were accessed using a method for the nitration[29] of loratadine that produces the two regioisomers **25** (major) and **28** (minor). For the synthesis of **11c** from **28**, the ethylcarbamate protecting group was replaced with a Boc protecting group (through intermediacy of **29**) to avoid the formation of side products observed in deprotection attempts of the ethylcarbamate in the last step (data not shown). Reduction of the nitro group of resulting intermediate **30** gave aniline **31**, which was converted to **32** *via in situ* diazotation and reaction with PhMgBr, based on a procedure of Barbero *et al.*[31] This alternative strategy was chosen because both acidic and basic Mills conditions on **31** were ineffective. Similarly, to obtain **11a**, compound **25** was converted to Boc-protected intermediate **27** *via* **26**. After reduction of the nitro group to **33** and a Mills reaction to **34**, Boc group deprotection afforded **11a**.

Rupatadine analogs (**12a–c**) were synthesized using two different routes (Scheme 2). For analogs **12a** (*para*) and **12b** (*meta*), the corresponding anilines **35** and **36** were coupled to PhNO *via* the Mills reaction under acidic conditions to afford azobenzenes **37** and **38**. These compounds were then oxidized to give aldehydes **39** and **40** using DMP or MnO_2, respectively. Reductive amination with desloratadine (**8**) yielded rupatadine analogs **12a** and **12b**. In contrast, synthesis of **12c** (*ortho*) required an alternative approach, as aldehyde formation from the corresponding azobenzene was unsuccessful. Instead, alkylation of desloratadine (**8**) with alkylbromide **41** gave nitro-compound **42**, which was reduced to aniline **43** and subjected to acidic Mills conditions to afford **12c**.

Photochemistry

The photochemical properties of the photoswitchable ligands (Table 1, Fig. S2–S10) were first characterized by UV-vis absorption spectroscopy. Spectra were recorded at a concentration of 25 μM in HBSS buffer containing 50% DMSO (Fig. S2–S10). Most compounds exhibit absorption patterns characteristic for azobenzenes and azopyridines.[32–34] The absorption maxima (λ_{max}) of the *trans* isomers are observed around 310–340 nm (π–π* absorption band). Of note is the π–π* transition band of **11c**, which is observed as a shoulder around 310 nm. Next to a potential effect of the *ortho*-Cl atom,[35] the absence of a comparable blue-shift in π–π* band for the related compound **11a** could highlight a steric effect on the absorption profile in **11c**. The λ_{max} values of the *cis* isomers are observed at 419–435 nm (*n*–π*

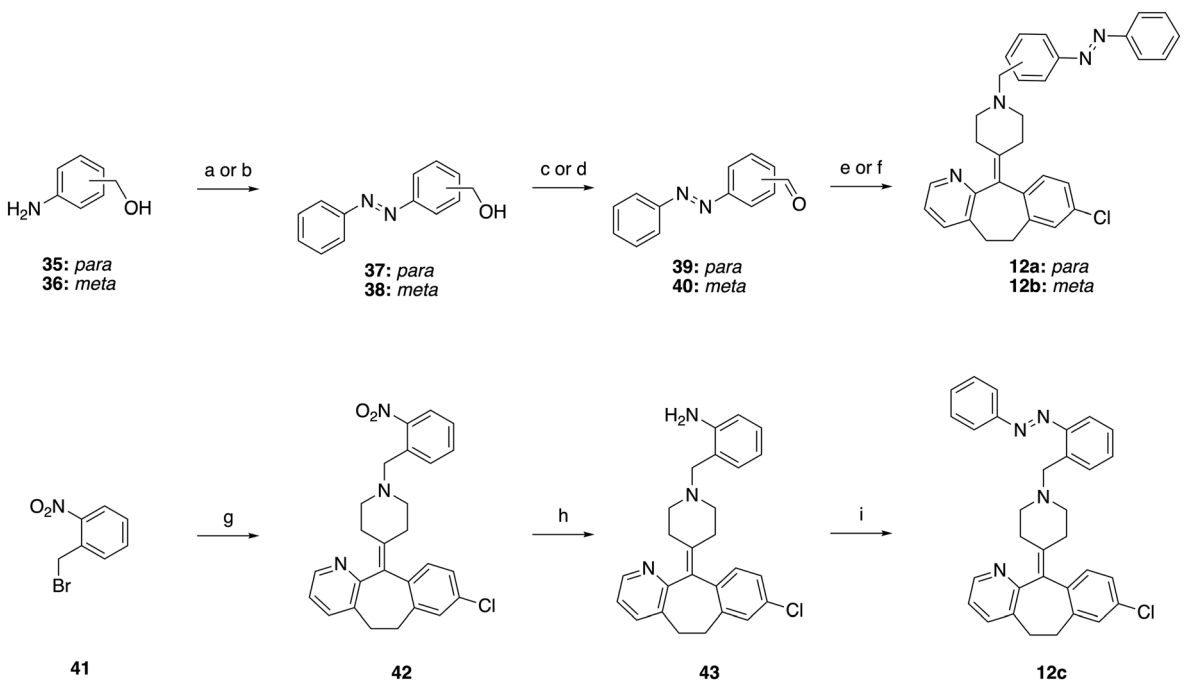

Scheme 2 Synthesis of **12a–c**. Reagents and conditions: (a) for **37**: PhNO, AcOH, rt, 66 h, 12%; (b) for **38**: PhNO, DCM, AcOH, rt, 18 h, 70%; (c) for **39**: DMP, DCM, rt, 1.5 h, 89%; (d) for **40**: MnO_2, DCM, rt, 2 h, 75%; (e) for **12a**: **8**, $NaBH(OAc)_3$, AcOH, DCE, rt, 16 h, 26%; (f) for **12b**: **8**, $NaBH(OAc)_3$, AcOH, DCM, rt, 2 h, 62%; (g) **8**, MeCN, K_2CO_3, reflux, 3 h, 91%; (h) Fe, NH_4Cl, 1,4-dioxane, EtOH, H_2O, 80 °C, 3 h, quantitative; (i) PhNO, PhMe, AcOH, 75 °C, 16 h, 12%.

Table 1 Photochemical parameters of **10a–c**, **11a–c** and **12a–c**

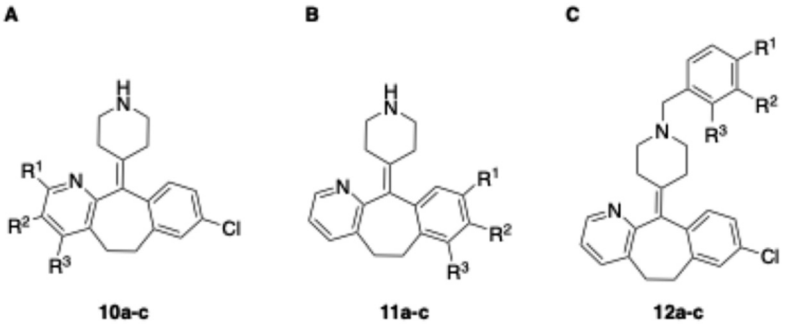

Compound	Structure	R^1	R^2	R^3	λ_{max} *trans*[a] (nm)	λ_{max} *cis*[a] (nm)	PSS_{cis} (area% *cis*)[b]	PSS_{trans} (area% *trans*)[b]	Approximate $t_{1/2}$[c]
10a	A	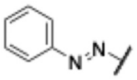	H	H	332	429	91	85	38 d
10b	A	H	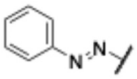	H	335	430	87	79	31 d
10c	A	H	H	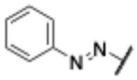	319	419	n.d.[d]	n.d.[d]	15 min
11a	B	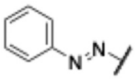	Cl	H	340	429	97	79	78 d
11b	B	H	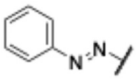	H	338	435	91	80	5 d
11c	B	H	Cl	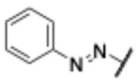	~310[e]	419	67	82	211 d
12a	C	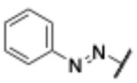	H	H	327	432	93	83	19 d
12b	C	H	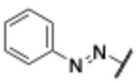	H	325	423	91	81	198 d
12c	C	H	H	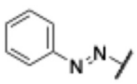	329	—	n.d.[d]	n.d.[d]	45 s

[a] Determined at 25 μM in HBSS buffer containing 50% DMSO. [b] Photostationary state area percentages either after illumination of *trans* isomer with 360 ± 20 nm at 10 mM in DMSO as determined by acidic LC-MS analysis at the isosbestic point, or after illumination of PSS_{cis} states with 434 ± 9 nm at 10 mM in DMSO as determined by acidic LC-MS analysis at the isosbestic point. [c] Thermal relaxation ($t_{1/2}$) of PSS_{cis} states in HBSS buffer containing 50% DMSO, as estimated by the method of Ahmed *et al.*[36] by extrapolating to 20 °C. Arrhenius plots are available in SI. [d] Photostationary state area percentages could not be determined by LC-MS analysis due to the small $t_{1/2}$ value. [e] Approximate value due to overlapping bands.

absorption band). Due to the short thermal half-life of **10c** and **12c** (*vide infra*), determination of the λ_{max} value of their *cis* isomer and quantification of their photostationary states (PSS) was not feasible. The *trans* to *cis* isomerization for all other compounds could be quantified upon illumination with 360 nm, resulting in PSS_{cis} values ranging from 87–97%. The exception was compound **11c**, which only reaches a moderate PSS_{cis} value of 67% (*vide supra*, Fig. S7C). Indeed, UV analysis (Fig. S7B) clearly shows that 360 nm is near an isosbestic point of **11c**. All compounds show expected PSS_{trans} values between 79–85% upon illumination with 434 nm. The approximated dark stabilities of these compounds in buffer vary substantially, with thermal half-lives ranging from seconds (**12c**) and minutes (**10c**) to days (**11b**, **12a**) and even months (**10a**, **10b**, **11a**, **11c**, **12b**).

Pharmacology

The affinities (pK_i values) of **10a–c**, **11a–c** and **12a–c** for the hH_1R were evaluated in competition radioligand-binding experiments with the labelled H_1R antagonist [^{3}H]mepyramine

(Table 2, Fig. S11–S13). For **10c** and **12c**, continuous illumination at 365 nm was used to counteract the short half-lives of their PSS_{cis} states, while for the other compounds PSS_{cis} states were obtained by pre-illumination with 360 nm. In the first series, featuring substitutions on the pyridine ring (**10a–c**), substitution on the 2-position (**10a**) provides a compound with high affinity for the *trans* isomer (pK_i = 8.3, template **8**: pK_i = 9.6) and a lower affinity in the PSS_{cis} state (pK_i = 7.8), resulting in a significant light-induced affinity shift of −0.5 log unit (*i.e.*, a 3.2-fold shift in affinity). Incorporation of an azobenzene at the 3-position (**10b**) is also well tolerated (pK_i *trans* = 8.7). However, a reduced light-induced affinity shift was observed between *trans*-**10b** and **10b**-PSS_{cis} (−0.3 log unit). Placement of the azobenzene on the 4-position (**10c**) reduces affinity for the *trans* isomer compared to **10a** and **10b**, providing high-nM affinities (pK_i **10c** = 6.8). However, **10c** shows no affinity shift upon photoisomerization, indicating that this position is not optimal for azobenzene placement. In the second series (**11a–c**), which involves substitution on the phenyl ring, *trans*-**11a** and *trans*-**11b** have comparable affinity to *trans*-**10c** (pK_i = 6.8). Noteworthy, **11b** shows a significant affinity shift (−0.6 log unit) between *trans* and $PSS_{cis.}$ In contrast, substitution at the 7-position (**11c**) results in a loss of affinity for hH_1R for either state ($pK_i < 6.0$), indicating that

Table 2 Human histamine H_1R binding affinity (pK_i) values and affinity shifts of **10a–c**, **11a–c** and **12a–c**

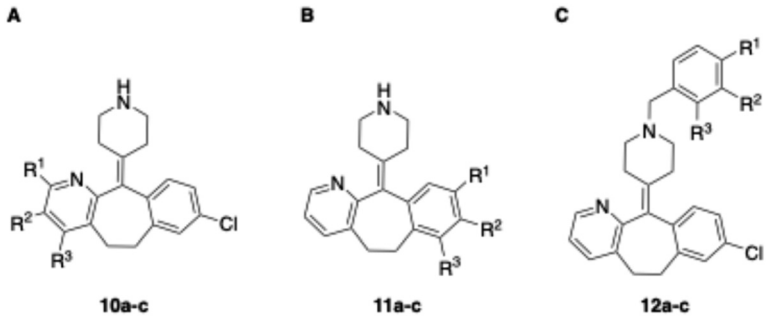

Compound number	Structure	R^1	R^2	R^3	pK_i *trans*[a]	pK_i PSS_{cis}[a]	pK_i shift[b]
8	A	H	H	H	9.6 ± 0.1	—	—
10a	A	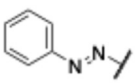	H	H	8.3 ± 0.2	7.8 ± 0.2	−0.5
10b	A	H	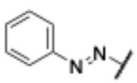	H	8.7 ± 0.1	8.4 ± 0.1	−0.3
10c	A	H	H	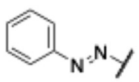	6.8 ± 0.0	6.8 ± 0.0[c]	0.0
11a	B	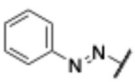	Cl	H	6.8 ± 0.2	6.6 ± 0.1	−0.2
11b	B	H	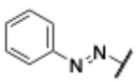	H	6.9 ± 0.0	6.3 ± 0.1	−0.6
11c	B	H	Cl	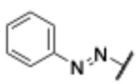	<6.0	<6.0	—
12a	C	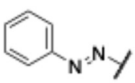	H	H	8.6 ± 0.5	8.5 ± 0.2	−0.1
12b	C	H	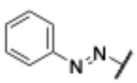	H	8.3 ± 0.1	8.2 ± 0.1	−0.1
12c	C	H	H	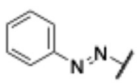	8.4 ± 0.2	8.3 ± 0.2[c]	−0.1

[a] Affinity (pK_i) values as obtained from radioligand competition experiments with [^{3}H]mepyramine. Values are mean ± SEM of n = 3 experiments, performed in triplicate. Competition binding curves are available in the SI. [b] Affinity shifts between PSS_{cis} and *trans* states are defined as pK_i PSS_{cis}–pK_i *trans*. [c] Continuous illumination at 365 nm was used during 4 h incubation at 25 °C.

this position is not suitable for azologization. The third series (**12a–c**), involving rupatadine analogs, provides high affinities for the *trans* isomers (pK_i = 8.3–8.6, template **9**: pK_i = 8.4, Fig. 1). This is in line with other reports showing that the piperidine of **8** can be substituted without eroding H_1R affinities.[24,37,38] However, none of the ligands **12a–c** shows an affinity shift upon photoisomerization, indicating that the *N*-substitution of **8** is not a viable strategy to achieve photochemical modulation of hH_1R. In all, the **10** and **12** series are generally more amenable to appending *trans*-azobenzene moieties while maintaining affinities, with only the **10** series also showing some appreciable affinity shifts upon photoisomerization. The **11** series notably suffers from reduction in H_1R affinity upon appending a *trans* azobenzene, although some members in this series show affinity shifts upon photoisomerization. In all, **10a** and **11b** demonstrate the most pronounced light-induced affinity shifts among the three series (−0.5 and −0.6, respectively). Notably, **10a** displays an approximately 25-fold higher H_1R affinity (pK_i *trans* = 8.3) compared to **11b** and therefore emerges as the most suitable photopharmacological H_1R ligand in this study.

Proposed binding mode of 10a

Molecular modelling using the recently disclosed cryo-EM structure of H_1R with **8** (PDB ID: 8X64)[25] was performed to gain insight in the observed affinities of *trans*- and *cis*-**10a**. We investigated whether both isomers could bind to H_1R in a similar fashion as desloratadine. Indeed, *trans*-**10a** adopts a conformation similar to that of desloratadine (Fig. 3A). In this docking pose, the key interactions of the protonated amine with $D107^{3.32}$ and of the pyridine nitrogen atom with $Y431^{6.52}$ are maintained. The azobenzene moiety is directed towards the solvent-exposed region. In contrast, no comparable docking poses could be identified for *cis*-**10a**. Instead, for *cis*-**10a** a binding mode was identified in which the desloratadine core was flipped 180 degrees in the binding pocket. In this binding mode *cis*-**10a** maintains the key interaction with $D107^{3.32}$ *via* its protonated amine but lacks the hydrogen bond interaction with $Y431^{6.52}$. The azobenzene moiety is buried deep in the pocket where it forms a π-stacking interaction with $W428^{6.48}$, while the chloro-substituted ring of the desloratadine core forms an arene-H interaction with $Y108^{3.33}$. These binding modes explain the reduced affinity of *cis*-**10a** compared to that of *trans*-**10a**, while also providing a rationale for the still appreciable affinity of *cis*-**10a** owing to the maintained key ionic interaction with $D107^{3.32}$ and the two newly formed interactions with $Y108^{3.33}$ and $W428^{6.48}$. Based on these findings, computer-aided approaches could help the design of the next generation of desloratadine-based photoswitchable ligands, for example by focusing on increasing the bulk on the peripheral phenyl ring of **10a**. These modifications may allow the *trans* isomer to maintain a similar binding mode to *trans*-**10a** as its azobenzene moiety is directed towards the solvent-exposed region, while the *cis* isomer in its inverted binding mode would experience steric clashes with the protein. This in turn would lower the affinity of the *cis* isomer and therefore improve the affinity shift.

Conclusion

Finding effective photoswitchable ligands for optical control of the hH_1R remains challenging, which may be attributed to the intrinsic flexibility of the orthosteric binding pocket of hH_1R. Here, a total of nine potential photoswitchable ligands for hH_1R was explored by performing an 'azoscan' on the antihistamine desloratadine (**8**). Late-stage regioselective installation of aniline groups on the aromatic rings of the desloratadine scaffold enabled azobenzene formation and overall an aromatic azoscan. This was supplemented by a concise series of *N*-functionalized derivatives. Most ligands show efficient *trans* to *cis* isomerization (PSS_{cis} > 87%) by using an illumination wavelength of 360 nm, except for **11c**

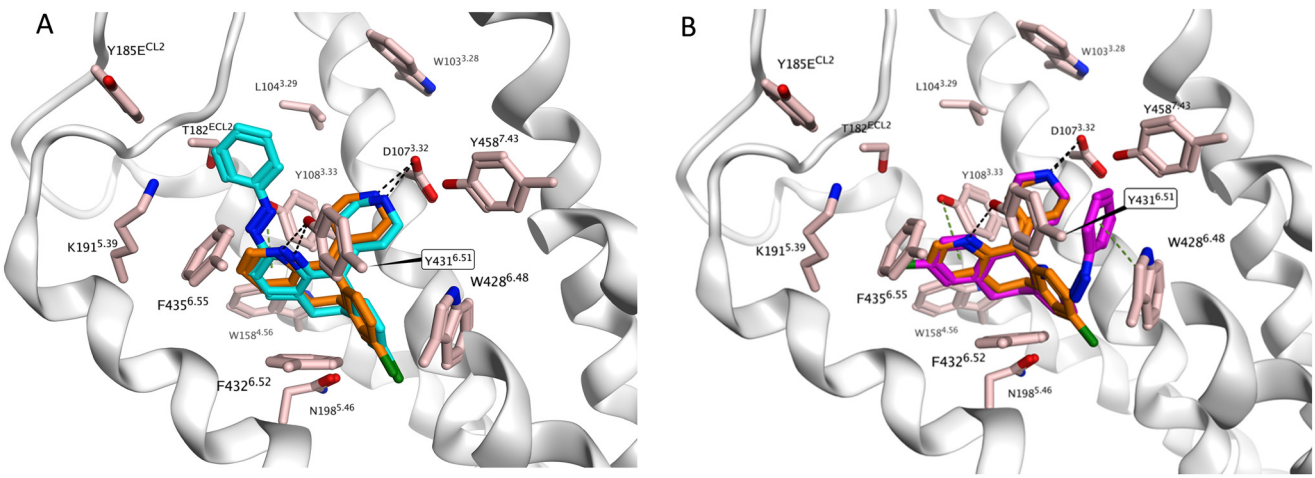

Fig. 3 Proposed binding mode of desloratadine (orange) in the H_1R binding pocket as determined by cryo-EM (PDB ID: 8X64)[25] in overlay with the docking pose of (A) *trans*-**10a** (cyan) and (B) *cis*-**10a** (purple).

(PSS_{cis} = 67%). Additionally, a wide range of half-lives was observed ranging from seconds to months. Pharmacological evaluation revealed marked differences in effect upon probing azobenzenes in the three regions of **8**, and only a few compounds show an appreciable light-induced H_1R affinity shift upon installation of an azobenzene. Two suitable positions, *i.e.* the 2-position (**10a**) and the 8-position (**11b**), were identified with similar H_1R affinity shifts between the *trans* and PSS_{cis} states. Of these, **10a** shows the most balanced profile (pK_i *trans* = 8.3, pK_i PSS_{cis} = 7.8). Molecular modeling studies indicate that the docking pose of *trans*-**10a** in H_1R shows good overlap with the binding mode of desloratadine, but that, in contrast, *cis*-**10a** adopts a flipped binding mode. Building on these findings, a light-induced H_1R affinity shift could potentially be improved by decorating the peripheral phenyl ring of the azobenzene of **10a**. Thus, photoswitchable ligand **10a** may provide a promising starting point for future development of improved hH_1R photoswitchable ligands.

Methods

Molecular modeling, synthetic chemistry, photochemistry, pharmacology and chemical analyses can be found in the SI.

Author contributions

LCPB: conceptualization, investigation, methodology, formal analysis, visualization, writing – original draft; IJ: conceptualization, investigation, methodology, formal analysis, writing – review & editing; DdV: investigation, formal analysis; TJN: investigation, formal analysis; NJH: conceptualization, investigation, formal analysis, writing – review & editing; SA: investigation, formal analysis; OPJL: visualization, supervision, writing – review & editing; IJPdE: supervision, writing – review & editing; HFV: supervision, funding acquisition, writing – review & editing; MW: supervision, funding acquisition, writing – original draft; RL: supervision, funding acquisition, writing – review & editing.

Conflicts of interest

There are no conflicts of interest to declare.

Data availability

Supplementary Information available: Detailed photochemical characterization, synthesis, chemical analyses, molecular modeling and pharmacological characterization. See DOI: https://doi.org/10.1039/D5MD00589B.

The data supporting this article have been included as part of the SI.

Acknowledgements

We acknowledge the Dutch Research Council (NWO) for financial support (OCENW.KLEIN.532, "Towards the next frontiers in GPCR photopharmacology"). We thank Hans Custers for acquiring HRMS analyses, Elwin Janssen for NMR assistance and Andrea van de Stolpe for support with the photochemistry equipment.

References

1 W. A. Velema, W. Szymanski and B. L. Feringa, Photopharmacology: Beyond Proof of Principle, *J. Am. Chem. Soc.*, 2014, **136**(6), 2178–2191, DOI: 10.1021/ja413063e.
2 Y. Liu, T. Wang and W. Wang, Photopharmacology and Photoresponsive Drug Delivery, *Chem. Soc. Rev.*, 2025, **54**, 5792–5835, DOI: 10.1039/d5cs00125k.
3 L. Josa-Culleré and A. Llebaria, In the Search for Photocages Cleavable with Visible Light: An Overview of Recent Advances and Chemical Strategies, *ChemPhotoChem*, 2021, **5**(4), 298–316, DOI: 10.1002/cptc.202000253.
4 M. J. Fuchter, On the Promise of Photopharmacology Using Photoswitches: A Medicinal Chemist's Perspective, *J. Med. Chem.*, 2020, **63**(20), 11436–11447, DOI: 10.1021/acs.jmedchem.0c00629.
5 J. Broichhagen, J. A. Frank and D. Trauner, A Roadmap to Success in Photopharmacology, *Acc. Chem. Res.*, 2015, **48**(7), 1947–1960, DOI: 10.1021/acs.accounts.5b00129.
6 P. Kobauri, F. J. Dekker, W. Szymanski and B. L. Feringa, Rational Design in Photopharmacology with Molecular Photoswitches, *Angew. Chem., Int. Ed.*, 2023, **62**(30), e202300681, DOI: 10.1002/anie.202300681.
7 K. Hüll, J. Morstein and D. Trauner, In Vivo Photopharmacology, *Chem. Rev.*, 2018, **118**(21), 10710–10747, DOI: 10.1021/acs.chemrev.8b00037.
8 J. S. Lorente, A. V. Sokolov, G. Ferguson, H. B. Schiöth, A. S. Hauser and D. E. Gloriam, GPCR Drug Discovery: New Agents, Targets and Indications, *Nat. Rev. Drug Discovery*, 2025, **2025**, 1–22, DOI: 10.1038/s41573-025-01139-y.
9 F. E. R. Simons and K. J. Simons, Histamine and H1-Antihistamines: Celebrating a Century of Progress, *J. Allergy Clin. Immunol.*, 2011, **128**(6), 1139–1150.e4, DOI: 10.1016/J.JACI.2011.09.005.
10 M. Ricart-Ortega, J. Font and A. Llebaria, GPCR Photopharmacology, *Mol. Cell. Endocrinol.*, 2019, **488**, 36–51, DOI: 10.1016/j.mce.2019.03.003.
11 S. Panarello, X. Rovira, A. Llebaria and X. Gómez-Santacana, Photopharmacology of G-Protein-Coupled Receptors, in *Molecular Photoswitches*, John Wiley & Sons, Ltd, 2022, vol. 2, pp. 921–944, DOI: 10.1002/9783527827626.ch37.
12 M. Wijtmans, I. Josimovic, H. F. Vischer and R. Leurs, Optical Control of Class A G Protein-Coupled Receptors with Photoswitchable Ligands, *Curr. Opin. Pharmacol.*, 2022, **63**, 102192, DOI: 10.1016/j.coph.2022.102192.
13 A. E. Berizzi and C. Goudet, Strategies and Considerations of G-Protein-Coupled Receptor Photopharmacology, *Adv. Pharmacol.*, 2020, **88**, 143–172, DOI: 10.1016/bs.apha.2019.12.001.
14 K. Rustler, S. Pockes and B. König, Light-Switchable Antagonists for the Histamine H 1 Receptor at the Isolated Guinea Pig Ileum, *ChemMedChem*, 2019, **14**(6), 636–644, DOI: 10.1002/cmdc.201800815.
15 R. A. Smits, H. D. Lim, B. Stegink, R. A. Bakker, I. J. P. De Esch and R. Leurs, Characterization of the Histamine H4 Receptor

Binding Site. Part 1. Synthesis and Pharmacological Evaluation of Dibenzodiazepine Derivatives, *J. Med. Chem.*, 2006, **49**(15), 4512–4516, DOI: **10.1021/jm051008s**.

16 S. Kuhne, A. J. Kooistra, R. Bosma, A. Bortolato, M. Wijtmans, H. F. Vischer, J. S. Mason, C. De Graaf, I. J. P. De Esch and R. Leurs, Identification of Ligand Binding Hot Spots of the Histamine H1 Receptor Following Structure-Based Fragment Optimization, *J. Med. Chem.*, 2016, **59**(19), 9047–9061, DOI: **10.1021/acs.jmedchem.6b00981**.

17 S. Kuhne, R. Bosma, A. J. Kooistra, R. Riemens, M. C. M. Stroet, H. F. Vischer, C. de Graaf, M. Wijtmans, R. Leurs and I. J. P. de Esch, Probing the Histamine H1 Receptor Binding Site to Explore Ligand Binding Kinetics, *J. Med. Chem.*, 2024, **68**, 448–464, DOI: **10.1021/acs.jmedchem.4c02043v**.

18 M. K. Nielsen, B. J. Shields, J. Liu, M. J. Williams, M. J. Zacuto and A. G. Doyle, Mild, Redox-Neutral Formylation of Aryl Chlorides through the Photocatalytic Generation of Chlorine Radicals, *Angew. Chem.*, 2017, **129**(25), 7297–7300, DOI: **10.1002/ange.201702079**.

19 A. Dumoulin, J. K. Matsui, Á. Gutiérrez-Bonet and G. A. Molander, Synthesis of Non-Classical Arylated C-Saccharides through Nickel/Photoredox Dual Catalysis, *Angew. Chem.*, 2018, **130**(22), 6724–6728, DOI: **10.1002/ange.201802282**.

20 D. F. Nippa, K. Atz, R. Hohler, A. T. Müller, A. Marx, C. Bartelmus, G. Wuitschik, I. Marzuoli, V. Jost, J. Wolfard, M. Binder, A. F. Stepan, D. B. Konrad, U. Grether, R. E. Martin and G. Schneider, Enabling Late-Stage Drug Diversification by High-Throughput Experimentation with Geometric Deep Learning, *Nat. Chem.*, 2024, **16**(2), 239–248, DOI: **10.1038/s41557-023-01360-5**.

21 Q. Wan, Z. W. Hou, X. R. Zhao, X. Xie and L. Wang, Organoelectrophotocatalytic C-H Silylation of Heteroarenes, *Org. Lett.*, 2023, **25**(6), 1008–1013, DOI: **10.1021/acs.orglett.3c00144**.

22 S. K. Kariofillis, B. J. Shields, M. A. Tekle-Smith, M. J. Zacuto and A. G. Doyle, Nickel/Photoredox-Catalyzed Methylation of (Hetero)Aryl Chlorides Using Trimethyl Orthoformate as a Methyl Radical Source, *J. Am. Chem. Soc.*, 2020, **142**(16), 7683–7689, DOI: **10.1021/jacs.0c02805**.

23 H. D. Lim, R. M. Van Rijn, P. Ling, R. A. Bakker, R. L. Thurmond and R. Leurs, Evaluation of Histamine H1-, H2-, and H3-Receptor Ligands at the Human Histamine H4 Receptor: Identification of 4-Methylhistamine as the First Potent and Selective H4 Receptor Agonist, *J. Pharmacol. Exp. Ther.*, 2005, **314**(3), 1310–1321, DOI: **10.1124/jpet.105.087965**.

24 R. Bosma, Z. Wang, A. J. Kooistra, N. Bushby, S. Kuhne, J. Van Den Bor, M. J. Waring, C. De Graaf, I. J. De Esch, H. F. Vischer, R. J. Sheppard, M. Wijtmans and R. Leurs, Route to Prolonged Residence Time at the Histamine H1 Receptor: Growing from Desloratadine to Rupatadine, *J. Med. Chem.*, 2019, **62**(14), 6630–6644, DOI: **10.1021/acs.jmedchem.9b00447**.

25 D Wang, Q. Guo, Z. Wu, M. Li, B. He, Y. Du, K. Zhang and Y. Tao, Molecular Mechanism of Antihistamines Recognition and Regulation of the Histamine H1 Receptor, *Nat. Commun.*, 2024, **15**(1), 1–10, DOI: **10.1038/s41467-023-44477-4**.

26 M. S. Lall, A. Bassyouni, J. Bradow, M. Brown, M. Bundesmann, J. Chen, G. Ciszewski, A. E. Hagen, D. Hyek, S. Jenkinson, B. Liu, R. S. Obach, S. Pan, U. Reilly, N. Sach, D. J. Smaltz, D. K. Spracklin, J. Starr, M. Wagenaar and G. S. Walker, Late-Stage Lead Diversification Coupled with Quantitative Nuclear Magnetic Resonance Spectroscopy to Identify New Structure-Activity Relationship Vectors at Nanomole-Scale Synthesis: Application to Loratadine, a Human Histamine H1Receptor Inverse Agonist, *J. Med. Chem.*, 2020, **63**(13), 7268–7292, DOI: **10.1021/acs.jmedchem.0c00483**.

27 W. Verbeet, Y. Husiev and S. Bonnet, Simple and Efficient Method for Mono- and Di-Amination of Polypyridine N-Oxides, *Eur. J. Org. Chem.*, 2024, **27**(14), e202400054, DOI: **10.1002/ejoc.202400054**.

28 H. Choi, W. S. Ham, P. van Bonn, J. Zhang, D. Kim and S. Chang, Mechanistic Approach Toward the C4-Selective Amination of Pyridines via Nucleophilic Substitution of Hydrogen, *Angew. Chem., Int. Ed.*, 2024, **63**(24), e202401388, DOI: **10.1002/anie.202401388**.

29 F. George Njoroge, B. Vibulbhan, P. Pinto, T. M. Chan, R. Osterman, S. Remiszewski, J. D. Rosario, R. Doll, V. Girijavallabhan and A. K. Ganguly, Highly Regioselective Nitration Reactions Provide a Versatile Method of Functionalizing Benzocycloheptapyridine Tricyclic Ring Systems: Application toward Preparation of Nanomolar Inhibitors of Farnesyl Protein Transferase, *J. Org. Chem.*, 1998, **63**(3), 445–451, DOI: **10.1021/jo971100z**.

30 F. George Njoroge, B. Vibulbhan, D. F. Rane, W. Robert Bishop, J. Petrin, R. Patton, M. S. Bryant, K. J. Chen, A. A. Nomeir, C. C. Lin, M. Liu, I. King, J. Chen, S. Lee, B. Yaremko, J. Dell, P. Lipari, M. Malkowski, Z. Li, J. Catino, R. J. Doll, V. Girijavallabhan and A. K. Ganguly, Structure-Activity Relationship of 3-Substituted N-(Pyridinylacetyl)-4- (8-Chloro-5,6-Dihydro-11H-Benzo[5,6]Cyclohepta[1,2-b]Pyridin-11-Ylidene)- Piperidine Inhibitors of Farnesyl-Protein Transferase: Design and Synthesis of in Vivo Active Antitumor Compounds, *J. Med. Chem.*, 1997, **40**(26), 4290–4301, DOI: **10.1021/jm970464g**.

31 M. Barbero, I. Degani, S. Dughera, R. Fochi and P. Perracino, Preparation of Diazenes by Electrophilic C-Coupling Reactions of Dry Arenediazonium o-Benzenedisulfonimides with Grignard Reagents, *Synthesis*, 1998, **1998**(09), 1235–1237, DOI: **10.1055/s-1998-6102**.

32 M. Nakagawa, M. Rikukawa, M. Watanabe, K. Sanui and N. Ogata, Photochromic, Electrochemical, and Photoelectrochemical Properties of Novel Azopyridinium Derivatives, *Bull. Chem. Soc. Jpn.*, 1997, **70**(4), 737–744, DOI: **10.1246/BCSJ.70.737**.

33 Y. Xu, C. Gao, J. Andréasson and M. Grøtli, Synthesis and Photophysical Characterization of Azoheteroarenes, *Org. Lett.*, 2018, **20**(16), 4875–4879, DOI: **10.1021/acs.orglett.8b02014**.

34 J. Otsuki and K. Narutaki, Photochromism of Phenylazopyridines and Its Application to the Fluorescence Modulation of Zinc–Porphyrins, *Bull. Chem. Soc. Jpn.*, 2004, **77**(8), 1537–1544, DOI: **10.1246/bcsj.77.1537**.

35 D. B. Konrad, G. Savasci, L. Allmendinger, D. Trauner, C. Ochsenfeld and A. M. Ali, Computational Design and Synthesis of a Deeply Red-Shifted and Bistable Azobenzene, *J. Am. Chem. Soc.*, 2020, **142**(14), 6538–6547, DOI: **10.1021/jacs.9b10430**.

36 Z. Ahmed, A. Siiskonen, M. Virkki and A. Priimagi, Controlling Azobenzene Photoswitching through Combined Ortho-Fluorination and -Amination, *Chem. Commun.*, 2017, **53**(93), 12520–12523, DOI: **10.1039/c7cc07308a**.
37 Y. Wang, J. Wang, Y. Lin, L. F. Si-Ma, D. H. Wang, L. G. Chen and D. K. Liu, Synthesis and Antihistamine Evaluations of Novel Loratadine Analogues, *Bioorg. Med. Chem. Lett.*, 2011, **21**(15), 4454–4456, DOI: **10.1016/j.bmcl.2011.06.012**.
38 Y. Lin, Y. Wang, L. F. Sima, D. H. Wang, X. H. Cao, L. G. Chen and B. Chen, Design, Synthesis and Biological Activity Evaluation of Desloratadine Analogues as H1 Receptor Antagonists, *Bioorg. Med. Chem.*, 2013, **21**(14), 4178–4185, DOI: **10.1016/j.bmc.2013.05.004**.